

Xin Chen

State Key Laboratory for Strength and Vibration
of Mechanical Structures,
Xi'an Jiaotong University,
Xi'an 710049, China;
Bioinspired Engineering and Biomechanics
Center (BEBC),
Xi'an Jiaotong University,
Xi'an 710049, China;
State Key Laboratory of Mechanics and Control
of Mechanical Structures,
Nanjing University of Aeronautics
and Astronautics,
Nanjing 210016, China
e-mail: xinchen@126.com

Moxiao Li

State Key Laboratory for Strength
and Vibration of Mechanical Structures,
Xi'an Jiaotong University,
Xi'an 710049, China;
Bioinspired Engineering and Biomechanics
Center (BEBC),
Xi'an Jiaotong University,
Xi'an 710049, China
e-mail: rebone_1992@163.com

Shaobao Liu

State Key Laboratory of Mechanics and Control
of Mechanical Structures,
Nanjing University of Aeronautics
and Astronautics,
Nanjing 210016, China;
The Key Laboratory of Biomedical Information
Engineering of Ministry of Education,
Xi'an Jiaotong University,
Xi'an 710049, China
e-mail: shaobao_liu@126.com

Fusheng Liu

State Key Laboratory for Strength and Vibration
of Mechanical Structures,
Xi'an Jiaotong University,
Xi'an 710049, China;
Bioinspired Engineering and Biomechanics
Center (BEBC),
Xi'an Jiaotong University,
Xi'an 710049, China
e-mail: liufusheng@foxmail.com

Guy M. Genin

The Key Laboratory of Biomedical Information
Engineering of Ministry of Education,
Xi'an Jiaotong University,
Xi'an 710049, China;
U.S. National Science Foundation Science
and Technology Center for Engineering
Mechanobiology,
Washington University,
St. Louis, MO 63130
e-mail: genin@wustl.edu

Translation of a Coated Rigid Spherical Inclusion in an Elastic Matrix: Exact Solution, and Implications for Mechanobiology

The displacement of relatively rigid beads within a relatively compliant, elastic matrix can be used to measure the mechanical properties of the matrix. For example, in mechanobiological studies, magnetic or reflective beads can be displaced with a known external force to estimate the matrix modulus. Although such beads are generally rigid compared to the matrix, the material surrounding the beads typically differs from the matrix in one or two ways. The first case, as is common in mechanobiological experimentation, is the situation in which the bead must be coated with materials such as protein ligands that enable adhesion to the matrix. These layers typically differ in stiffness relative to the matrix material. The second case, common for uncoated beads, is the situation in which the beads disrupt the structure of the hydrogel or polymer, leading to a region of enhanced or reduced stiffness in the neighborhood of the bead. To address both cases, we developed the first analytical solution of the problem of translation of a coated, rigid spherical inclusion displaced within an isotropic elastic matrix by a remotely applied force. The solution is applicable to cases of arbitrary coating stiffness and size of the coating. We conclude by discussing applications of the solution to mechanobiology. [DOI: 10.1115/1.4042575]

Keywords: translation of an inclusion, coated inclusion, force–displacement relationship, magnetic bead rheometry

¹Corresponding authors.

Contributed by the Applied Mechanics Division of ASME for publication in the JOURNAL OF APPLIED MECHANICS. Manuscript received December 12, 2018; final manuscript received January 10, 2019; published online March 5, 2019. Assoc. Editor: Yashashree Kulkarni.

Feng Xu¹

Bioinspired Engineering and Biomechanics
Center (BEB),
Xi'an Jiaotong University,
Xi'an 710049, China;
The Key Laboratory of Biomedical Information
Engineering of Ministry of Education,
Xi'an Jiaotong University,
Xi'an 710049, China
e-mail: fengxu@mail.xjtu.edu.cn

Tian Jian Lu¹

State Key Laboratory for Strength and Vibration
of Mechanical Structures,
Xi'an Jiaotong University,
Xi'an 710049, China;
State Key Laboratory of Mechanics
and Control of Mechanical Structures,
Nanjing University of Aeronautics
and Astronautics,
Nanjing 210016, China;
Nanjing Center for Multifunctional Lightweight
Materials and Structures (MLMS),
Nanjing University of Aeronautics
and Astronautics,
Nanjing 210016, China
e-mail: tjlu@mail.xjtu.edu.cn

1 Introduction

Tracking the displacements of a relatively rigid particle embedded within an elastic medium can be used to estimate the elastic modulus of that medium. The idea is that, by tracking the displacement of the sphere in response to a known force, one can estimate the elastic properties of the medium in which the sphere is embedded. This technique was first developed in the 1920s and applied to the elastic properties of cells and gels [1]; however, the models to which the experimental results were fit did not enable the estimation of elastic moduli. The first exact solutions of the theory of linear elasticity that enabled predictions of elastic moduli became available half a century later (Refs. [2,3] are English translation editions of these Russian works), as described in Sec. 2. The technique is now fairly standard, and a broad range of biological stiffness assays rely on tracking the motion of relatively rigid spherical beads by known magnetic or optical forces [4]. Additionally, these responses of rigid beads underlie the mechanics of magneto-elastic materials [5], and analogous responses are important in geo-mechanics [6].

However, across this entire range of applications, a common occurrence is that an interphase exists between the particle and the matrix. From the perspective of biomaterials and engineering composites, a coating must often be placed on the outside of the bead to ensure its adhesion to the matrix [7]. For example, in magnetic hydrogels, a protein peptide linker must often be placed on the exterior of the bead to ensure adhesion [8]. From the perspective of polymer and soil mechanics, rigid spheres can cause local compaction of matrix material. Additionally, sufficiently small spheres can act as “fillers” that disrupt the structure of a polymer [9]. These ligand layers, compacted layers, and disrupted layers typically differ in elastic properties relative to the matrix material, and the classical solutions available for interpretation of bead translation experiments are not applicable.

We therefore developed the first analytical solution of the problem of translation of a coated, rigid spherical inclusion displaced within an isotropic elastic matrix by a remotely applied force. We solved for the problem for a range of interactions between the particle and coating ranging from fully bonded to frictionless, and extended the solution to the case of multiple, interacting inclusions.

2 Background and Problem Statement

The mathematical analog of the rigid sphere inclusion translation problem dates back to an elastostatics problem solved by Robin in 1886 [10]. In the theory of elasticity, Lurie solved the problem of translation of a rigid ellipsoid [3,11]. Subsequently, the problem for some specific cases was solved. For example, Selvadurai developed the solution for a rigid sphere in an incompressible matrix [12], Zureick presented an analogous solution for the case of a transversely isotropic matrix [13], and Selvadurai considered the case of a frictionless “bilateral” interface between the inclusion and the matrix [14]. Following Kupradze [2] and Lurie and Belyaev [3], the rigid inclusion translation problem considered in the present study is referred to as Robin’s problem.

Although many biomaterials *in vivo* are anisotropic, the target applications we envision for our approach are *in vitro* systems for which isotropy is a good approximation such as hydrogels [15]. We therefore focus on only isotropic solids in this paper.

Note that for techniques based on spherical harmonics, the shear modulus G is typically more convenient to use than Young’s modulus $E = 2G(1 + \nu)$, where ν is Poisson’s ratio. This has been the case in nearly all previous theoretical literature on related problems [3,12,14,16], and in this paper, we also use shear modulus to describe the problem and express the solution.

A typical experiment involves applying a magnetic force F to an isolated rigid sphere of radius R_i that is embedded in an infinite, isotropic, linear elastic matrix of shear modulus G_m and measuring the displacement U in the direction of F . Without losing generality, we assume that both the force F and the displacement U are directed along the direction of the z -axis (Fig. 1). The effective shear modulus measured is then given by

$$G_{\text{eff}} = \frac{F/\pi R_i^2}{U/R_i} \quad (1)$$

Thereafter, the challenge is to relate G_{eff} to G_m using an exact solution from the theory of linear elasticity. For a noncoated

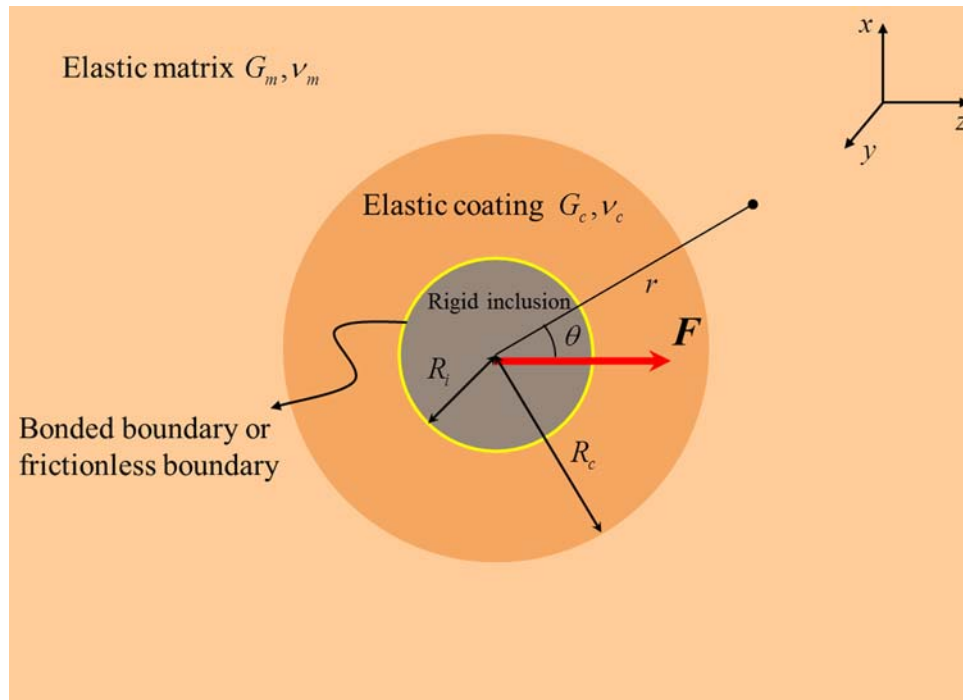


Fig. 1 Schematic figure of the problem. A rigid spherical inclusion with an elastic coating is imbedded in an infinite linear elastic matrix. G_m (N/m^2) and ν_m are the shear modulus and Poisson ratio of the matrix. G_c (N/m^2) and ν_c are the shear modulus and Poisson ratio of the coating, respectively. An external force with magnitude F translates the rigid inclusion and deforms the matrix and coating. The boundary between the inclusion and coating is constraint or frictionless, while the coating is perfectly bonded to the matrix.

sphere in an elastic matrix, the two are related by $\eta(\nu_m)$ that is a function only of the Poisson ratio ν_m of the matrix:

$$G_m = \eta(\nu_m) G_{\text{eff}} \quad (2)$$

The most important linear elasticity solution for interpretation of these experiments is the solution of Robin's problem [16,17] for a sphere that is perfectly adhered to the matrix, for which

$$\eta_{\text{bonded}}(\nu_m) = \frac{5 - 6\nu_m}{24(1 - \nu_m)} \quad (3)$$

which has the range $1/6 \leq \eta_{\text{bonded}}(\nu_m) \leq 11/48$.

For the case of a frictionless "bilateral" interface between the sphere and the matrix, which has an approximate frictionless boundary condition that will be discussed below, Selvadurai [14] derived the below expression:

$$\eta_{\text{unbonded}}(\nu_m) = \frac{7 - 8\nu_m}{24(1 - \nu_m)} \quad (4)$$

which has the range $1/4 \leq \eta_{\text{unbonded}} \leq 5/16$.

The relationship between G_m and G_{eff} becomes nonlinear and more complicated when a rigid spherical inclusion with an elastic coating is considered (Fig. 1). To arrive at the expression, we studied a rigid sphere of radius R_i with an elastic, concentric coating of outer radius R_c . Considering the rotational symmetry of the problem, we use a polar coordinate system. The origin of the system is set as the center of the rigid inclusion, while the $\theta = 0$ direction is set along the direction of the z -axis, i.e., the direction of the external force F . We also assumed F to be sufficiently small that the coating and matrix could be described by small strain linear elasticity.

2.1 Governing Equations. Within the framework of linear elasticity, the equations governing matrix deformation are

$$\begin{aligned} \boldsymbol{\varepsilon}^{(m)} &= \frac{1}{2}(\nabla \mathbf{u}^{(m)} + \mathbf{u}^{(m)} \nabla) \\ \boldsymbol{\sigma}^{(m)} &= 2G_m \left[\frac{\nu_m}{1 - 2\nu_m} \text{tr}(\boldsymbol{\varepsilon}^{(m)}) + \boldsymbol{\varepsilon}^{(m)} \right] \\ \nabla \cdot \boldsymbol{\sigma}^{(m)} &= 0 \end{aligned} \quad (5)$$

where $\mathbf{u}^{(m)}$, $\boldsymbol{\varepsilon}^{(m)}$, and $\boldsymbol{\sigma}^{(m)}$ are the displacement, strain, and stress in the matrix, respectively, and G_m (N/m^2) and ν_m are the shear modulus and Poisson ratio of the matrix material, respectively.

The equations governing the response of the coating are

$$\begin{aligned} \boldsymbol{\varepsilon}^{(c)} &= \frac{1}{2}(\nabla \mathbf{u}^{(c)} + \mathbf{u}^{(c)} \nabla) \\ \boldsymbol{\sigma}^{(c)} &= 2G_c \left[\frac{\nu_c}{1 - 2\nu_c} \text{tr}(\boldsymbol{\varepsilon}^{(c)}) + \boldsymbol{\varepsilon}^{(c)} \right] \\ \nabla \cdot \boldsymbol{\sigma}^{(c)} &= 0 \end{aligned} \quad (6)$$

where $\mathbf{u}^{(c)}$, $\boldsymbol{\varepsilon}^{(c)}$, and $\boldsymbol{\sigma}^{(c)}$ are the displacement, strain, and stress in the coating, respectively, and G_c (N/m^2) and ν_c are the shear modulus and the Poisson ratio of the coating material, respectively.

2.2 Boundary Conditions. Two sets of boundary conditions were considered. In the first, the connection between the coating and the sphere was treated as perfectly bonded, and in the second it was treated as frictionless. In both cases, the coating was perfectly bonded to the matrix material, so that the displacement and stress fields were continuous:

$$\mathbf{u}_c|_{r=R_c} = \mathbf{u}_m|_{r=R_c}, \quad \boldsymbol{\sigma}_c|_{r=R_c} = \boldsymbol{\sigma}_m|_{r=R_c} \quad (7)$$

For the case of a perfectly bonded sphere-coating interface, the boundary condition for the sphere-coating interface was

$$u_r^{(c)}|_{r \rightarrow R_i} = U \cos \theta, \quad u_\theta^{(c)}|_{r \rightarrow R_i} = -U \sin \theta \quad (8)$$

For the case of a frictionless sphere-coating interface, an approximate, smooth bilateral interaction was used, which assumed sufficient normal contact stresses to prevent separation at the interface; this is used widely for analogous problems [18,19]. The boundary condition was thus

$$u_r^{(c)}|_{r \rightarrow R_i} = U \cos \theta, \quad \sigma_{r\theta}^{(c)}|_{r \rightarrow R_i} = 0 \quad (9)$$

In the far field, the matrix was free from load, so that

$$\mathbf{u}^{(m)}|_{r \rightarrow \infty} = \mathbf{0} \quad (10)$$

3 Solution of the Problem

In addition to experimental [4] and simulation methods [20], two approaches have been developed for solving equations such as Eqs. (5)–(10) for the noncoated spherical inclusion problem. Walpole [21] and Kachanov et al. [22] used a generalized Eshelby equivalent inclusion approach [23], while Selvadurai and others [14,24] used Legendre polynomial-based solutions. We adopted the latter approach and wrote the solution as

$$\begin{aligned} u_r &= \sum_{n=0}^{\infty} \left[\frac{A_n}{r^n} n(n+3-4\nu) - \frac{B_n(n+1)}{r^{n+2}} \right] P_n(\cos \theta) \\ &+ \sum_{n=-\infty}^{-1} \left[\frac{A_n}{r^n} n(n+3-4\nu) - \frac{B_n(n+1)}{r^{n+2}} \right] P_{-n-1}(\cos \theta) \\ u_\theta &= \sum_{n=0}^{\infty} \left[\frac{A_n}{r^n} (-n+4-4\nu) + \frac{B_n}{r^{n+2}} \right] \frac{\partial}{\partial \theta} P_n(\cos \theta) \\ &+ \sum_{n=-\infty}^{-1} \left[\frac{A_n}{r^n} (-n+4-4\nu) + \frac{B_n}{r^{n+2}} \right] \frac{\partial}{\partial \theta} P_{-n-1}(\cos \theta) \end{aligned} \quad (11)$$

where ν is the Poisson ratio of the coating or matrix and $P_n(\cos \theta)$ is the Legendre polynomial of rank n .

3.1 Perfectly Bonded Inclusion and Coating. For the perfectly bonded case, with boundary conditions represented by Eqs. (7), (8), and (10), the displacement fields within the coating could be written as

$$\begin{aligned} u_r^{(c)} &= \cos \theta \left[A_0^{(c)} - 2(1-4\nu_c)A_1^{(c)}r^2 + 4(1-\nu_c)\frac{A_2^{(c)}}{r} - 2\frac{A_3^{(c)}}{r^3} \right] \\ u_\theta^{(c)} &= -\sin \theta \left[A_0^{(c)} + (6-4\nu_c)A_1^{(c)}r^2 + (3-4\nu_c)\frac{A_2^{(c)}}{r} + \frac{A_3^{(c)}}{r^3} \right] \end{aligned} \quad (12)$$

and those in the matrix as

$$\begin{aligned} u_r^{(m)} &= \cos \theta \left[4(1-\nu_m)\frac{A_2^{(m)}}{r} - 2\frac{A_3^{(m)}}{r^3} \right] \\ u_\theta^{(m)} &= -\sin \theta \left[(3-4\nu_m)\frac{A_2^{(m)}}{r} + \frac{A_3^{(m)}}{r^3} \right] \end{aligned} \quad (13)$$

where $A_0^{(c)}, A_1^{(c)}, A_2^{(c)}, A_3^{(c)}, A_2^{(m)}, A_3^{(m)}$ are coefficients shown in Appendix A. Then, the stress field in the coating was

$$\begin{aligned} \sigma_{rr}^{(c)} &= -4G_c \cos \theta \left[2(1+\nu_c)A_1^{(c)}r - (-2+\nu_c)\frac{A_2^{(c)}}{r^2} - 3\frac{A_3^{(c)}}{r^4} \right] \\ \sigma_{r\theta}^{(c)} &= -2G_c \sin \theta \left[2(1+\nu_c)A_1^{(c)}r + (-1+2\nu_c)\frac{A_2^{(c)}}{r^2} - 3\frac{A_3^{(c)}}{r^4} \right] \end{aligned} \quad (14)$$

and that in the matrix was

$$\begin{aligned} \sigma_{rr}^{(m)} &= -4G_m \cos \theta \left[(-2+\nu_m)\frac{A_2^{(m)}}{r^2} - 3\frac{A_3^{(m)}}{r^4} \right] \\ \sigma_{r\theta}^{(m)} &= -2G_m \sin \theta \left[(-1+2\nu_m)\frac{A_2^{(m)}}{r^2} - 3\frac{A_3^{(m)}}{r^4} \right] \end{aligned} \quad (15)$$

The force F of the inclusion must balance the boundary traction on the inclusion-coating interface. Because of the axial-symmetry of the problem, summation of the boundary force on the inclusion-coating interface in the direction of the applied force ($\theta=0$) could be written as

$$F = 2\pi R_i^2 \int_0^\pi (\sigma_{rr}^{(c)} \cos \theta - \sigma_{r\theta}^{(c)} \sin \theta) \sin \theta d\theta \quad (16)$$

Substituting from Eq. (15) yielded

$$F = 16\pi A_2^{(c)}(-1+\nu_c)G_c \quad (17)$$

which could be rewritten as

$$\frac{G_{\text{eff}}}{G_m} = \frac{S\beta(X_1 + X_2\beta)}{X_3 + X_4\beta + X_5\beta^2} \quad (18)$$

where

$$\begin{aligned} \alpha &= \frac{R_c}{R_i}, \quad \beta = \frac{G_c}{G_m} \\ S &= 48\alpha(1-\nu_m)(1-\nu_c) \\ X_1 &= (\alpha^5 - 1)(4 - 6\nu_c) \\ X_2 &= 4 - 6\nu_c + \alpha^5(1 + \nu_c) \\ X_3 &= (\alpha - 1)^2(1 - \nu_m)[4(1 + \alpha^4)(2 - 3\nu_c)(5 - 6\nu_c) \\ &+ \alpha(1 + \alpha^2)(35 - 108\nu_c + 72\nu_c^2) \\ &+ 6\alpha^2(5 - 18\nu_c + 12\nu_c^2)] \\ X_4 &= (-1 + \alpha)\{4(2 - 3\nu_c)(10 - 11\nu_m - 11\nu_c + 12\nu_m\nu_c) \\ &+ \alpha(1 + \alpha)[35 - 43\nu_m - 4\nu_c(5 - 6\nu_m)(5 - 3\nu_c)] \\ &+ \alpha^3(1 + \alpha)[45 - 53\nu_m - 4\nu_c(5 - 6\nu_m)(5 - 3\nu_c)] \\ &+ 2\alpha^5(1 - \nu_m)(1 + \nu_c)(5 - 6\nu_c)\} \\ X_5 &= 2(5 - 6\nu_m)(1 - \nu_c)[2(2 - 3\nu_c) + \alpha^5(1 + \nu_c)] \end{aligned} \quad (19)$$

Although the relationship is in general nonlinear and must be solved numerically, Eq. (18) reduces to the simple form of the solution of Robin's problem (Eq. (3)) in all of the appropriate cases, including a coating with no material mismatch ($\nu_c = \nu_m$, $G_c = G_m$) and a coating with no thickness ($R_c/R_i = 1$). In the case of no material mismatch, this is seen in Fig. 2. In the limit when $R_c/R_i \rightarrow 1$, we observe that

$$\lim_{\alpha \rightarrow 0} X_1 = 0, \quad \lim_{\alpha \rightarrow 0} X_3 = 0, \quad \lim_{\alpha \rightarrow 0} X_4 = 0$$

from which it follows that

$$\begin{aligned} \lim_{\alpha \rightarrow 1} \frac{G_{\text{eff}}}{G_m} &= \lim_{\alpha \rightarrow 1} \frac{SX_2}{X_5} \\ &= \lim_{\alpha \rightarrow 1} \frac{48\alpha(1-\nu_m)(1-\nu_c)[4-6\nu_c+\alpha^5(1+\nu_c)]}{2(5-6\nu_m)(1-\nu_c)[2(2-3\nu_c)+\alpha^5(1+\nu_c)]} \\ &= \frac{24(1-\nu_m)}{5-6\nu_m} \end{aligned}$$

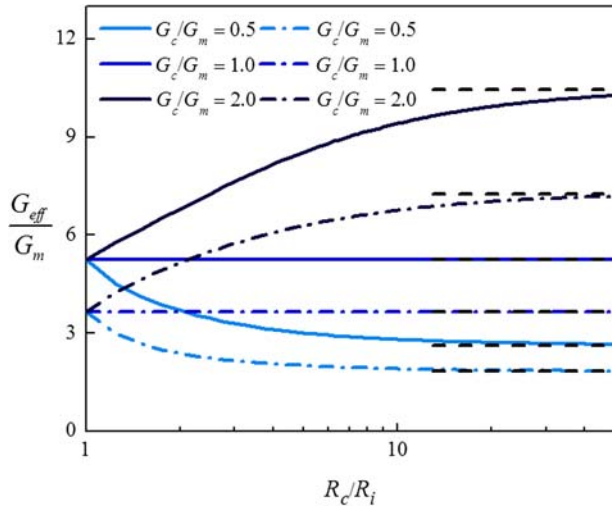


Fig. 2 The influence of coating radius on the effective modulus. The effective modulus is defined as $G_{\text{eff}} = ((F/\pi R_i^2)/(U/R_i))$. Different trends represent different stiffness of the coating. The solid lines represent the cases of bonded boundary, and the dash dot lines represent the cases of frictionless boundary. As R_c/R_i increases, each line approaches an asymptote (dashed lines). The dashed lines were calculated using the solutions given in Ref. [14] for the case of a rigid inclusion translation in an infinite solid which has the same material properties (i.e., shear modulus G_c and Poisson ratio ν_c) as the coating. $\nu_c = 0.3$ and $\nu_m = 0.3$ were chosen in this figure.

or can be written in an alternative way as

$$G_m = \frac{5 - 6\nu_m}{24(1 - \nu_m)} G_{\text{eff}}$$

This result is the same as that given by Eqs. (2) and (3).

Similarly, as expected, Eq. (18) yields, for an infinitely thick coating,

$$\frac{G_c}{G_{\text{eff}}} = \eta_{\text{bonded}}(\nu_c) \quad (20)$$

which is the solution of Robin's problem with the coating properties substituted for the matrix properties. For a rigid coating ($G_c/G_m \rightarrow \infty$), the expression again recovers the solution of the classic Robin problem, except with the sphere radius replaced by R_c to represent a larger radius sphere.

3.2 Frictionless Inclusion-Coating Interface. For the frictionless case, with boundary conditions represented by Eqs. (7), (9), and (10), the displacement fields within the coating could be written as

$$u_r^{(c)} = \cos \theta \left[B_0^{(c)} - 2(1 - 4\nu_c)B_1^{(c)}r^2 + 4(1 - \nu_c)\frac{B_2^{(c)}}{r} - 2\frac{B_3^{(c)}}{r^3} \right] \quad (21)$$

$$u_\theta^{(c)} = -\sin \theta \left[B_0^{(c)} + (6 - 4\nu_c)B_1^{(c)}r^2 + (3 - 4\nu_c)\frac{B_2^{(c)}}{r} + \frac{B_3^{(c)}}{r^3} \right]$$

and the displacement fields in the matrix as

$$u_r^{(m)} = \cos \theta \left[4(1 - \nu_m)\frac{B_2^{(m)}}{r} - 2\frac{B_3^{(m)}}{r^3} \right] \quad (22)$$

$$u_\theta^{(m)} = -\sin \theta \left[(3 - 4\nu_m)\frac{B_2^{(m)}}{r} + \frac{B_3^{(m)}}{r^3} \right]$$

where $B_0^{(c)}, B_1^{(c)}, B_2^{(c)}, B_3^{(c)}, B_2^{(m)}$, and $B_3^{(m)}$ are coefficients shown in Appendix A. The stress field in the coating was then

$$\sigma_{rr}^{(c)} = -4G_c \cos \theta \left[2(1 + \nu_c)B_1^{(c)}r - (-2 + \nu_c)\frac{B_2^{(c)}}{r^2} - 3\frac{B_3^{(c)}}{r^4} \right] \quad (23)$$

$$\sigma_{r\theta}^{(c)} = -2G_c \sin \theta \left[2(1 + \nu_c)B_1^{(c)}r + (-1 + 2\nu_c)\frac{B_2^{(c)}}{r^2} - 3\frac{B_3^{(c)}}{r^4} \right]$$

and that in the matrix was

$$\sigma_{rr}^{(m)} = -4G_m \cos \theta \left[-(-2 + \nu_m)\frac{B_2^{(m)}}{r^2} - 3\frac{B_3^{(m)}}{r^4} \right] \quad (24)$$

$$\sigma_{r\theta}^{(m)} = -2G_m \sin \theta \left[(-1 + 2\nu_m)\frac{B_2^{(m)}}{r^2} - 3\frac{B_3^{(m)}}{r^4} \right]$$

Following Eq. (16), the force could be written as

$$F = 16\pi B_2^{(c)}(-1 + \nu_c)G_c \quad (25)$$

and the effective modulus could be written as

$$\frac{G_{\text{eff}}}{G_m} = \frac{48\alpha\beta(-1 + \nu_m)(1 - \nu_c)(Y_1 + Y_2\beta)}{Y_3 + Y_4\beta + Y_5\beta^2} \quad (26)$$

where

$$Y_1 = 1 + \nu_c + 2\alpha^5(2 - 3\nu_c)$$

$$Y_2 = (\alpha^5 - 1)(1 + \nu_c)$$

$$Y_3 = (\alpha - 1)(1 - \nu_m)[2(1 + \nu_c)(5 - 6\nu_c) + \alpha(1 + \alpha)(1 - 20\nu_c + 24\nu_c^2) + \alpha^3(1 + \alpha)(11 - 40\nu_c + 24\nu_c^2) + 4\alpha^5(2 - 3\nu_c)(7 - 8\nu_c)] \quad (27)$$

$$Y_4 = 2(1 + \nu_c)(10 - 11\nu_m - 11\nu_c + 12\nu_m\nu_c) - 9\alpha(1 - \nu_m)(1 + 2\nu_c - 4\nu_c^2) + 10\alpha^3(1 - \nu_m)(1 - 2\nu_c) + \alpha^5(35 - 43\nu_m - 98\nu_c + 118\nu_m\nu_c + 72\nu_c^2 - 84\nu_m\nu_c^2) + 2\alpha^6(1 - \nu_m)(1 + \nu_c)(7 - 8\nu_c)$$

$$Y_5 = 2(\alpha^5 - 1)(5 - 6\nu_m)(1 - \nu_c)(1 + \nu_c)$$

As above, Eq. (26) reduces to the solution of the classic Robin problem (Eq. (4)) in the appropriate limits, including a coating with no material mismatch ($\nu_c = \nu_m, G_c = G_m$). Reduction to the limiting case of no material match is demonstrated by the numerical results shown in Fig. 2. In the limit when $R_c/R_i \rightarrow 1$, we observe that

$$\lim_{\alpha \rightarrow 0} Y_2 = 0, \quad \lim_{\alpha \rightarrow 0} Y_3 = 0, \quad \lim_{\alpha \rightarrow 0} Y_5 = 0$$

from which

$$\lim_{\alpha \rightarrow 1} \frac{G_{\text{eff}}}{G_m} = \lim_{\alpha \rightarrow 1} \frac{48\alpha(-1 + \nu_m)(1 - \nu_c)Y_1}{Y_4} = \frac{48(-1 + \nu_m)(1 - \nu_c)[1 + \nu_c + 2(2 - 3\nu_c)]}{10(7 - 8\nu_m)(1 - \nu_c)^2} = \frac{24(1 - \nu_m)}{7 - 8\nu_m}$$

or equivalently

$$G_m = \frac{7 - 8\nu_m}{24(1 - \nu_m)} G_{\text{eff}}$$

This solution is the same as that given by Eqs. (4) and (5).

4 Results and Discussion

The expressions derived in Sec. 3 indicated that the stiffness and thickness of the coating influences the force–displacement relationships. After exploring this effect, we estimated the stiffness of the coating from these force–displacement relationships.

4.1 Force–Displacement Relationships. Studying Eqs. (18) and (26) as a function of the normalized coating thickness R_c/R_i (Fig. 2(a)) for the case of $\nu_c = \nu_m = 0.3$ revealed an asymptote in G_{eff}/G_m for thin coatings ($R_c/R_i \rightarrow 1$), which is independent of whether the inclusion-coating interface was bonded or frictionless. This indicated that a coating could be neglected provided that the coating thickness is sufficiently thin. G_{eff}/G_m increased for stiff coatings ($G_c/G_m > 1$) and decreased for compliant coatings ($G_c/G_m < 1$), indicating that coatings that are stiff compared to the matrix attenuate translation of the sphere, while coatings that are compliant compared to the matrix enhance it. Comparison of the two interfacial conditions revealed that the constrained boundary provides more resistance to bead motion in all cases. As R_c/R_i increases, each line approaches a limit calculated by the classical solutions [14,21] of Robin’s problem, which means the translation behavior of a rigid inclusion coated by a thick coating is similar as the inclusion translation in an infinite matrix with shear modulus G_c and Poisson ratio ν_c .

Studying these equations as a function of the relative coating modulus G_c/G_m (Fig. 3) again revealed that G_{eff}/G_m increases with increasing G_c/G_m and that the constrained boundary condition increases the resistance to bead motion. G_{eff}/G_m approaches an asymptote for G_c/G_m sufficiently large that the coating approximates a rigid sphere of radius R_c . In that limit, the sphere-coating boundary condition does not affect the solution, and the solution approaches the solution [14,21] of Robin’s problem for a sphere of radius R_c . As expected, the solutions reduced to the solution [14,21] of Robin’s problem for a sphere of radius R_i for the case of a coating with no material mismatch ($G_c = G_m$, $\nu_c = \nu_m$). G_{eff}/G_m approaches 0 for coatings approximating a cavity ($G_c/G_m \rightarrow 0$).

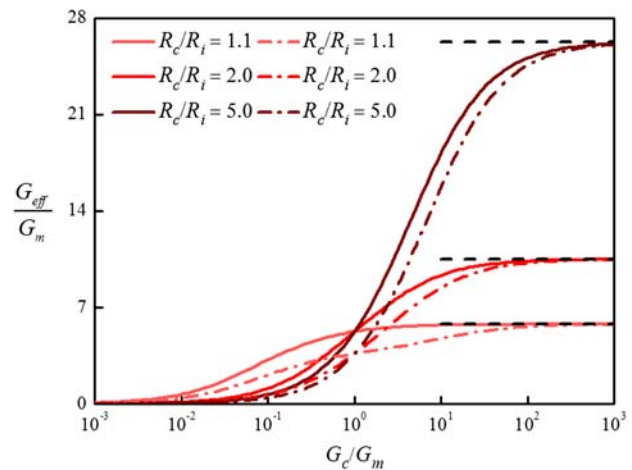


Fig. 3 The influence of coating stiffness on the effective modulus. The effective modulus is defined as $G_{\text{eff}} = ((F/\pi R_i^2)/(U/R_i))$. Different trends represent different radii of the coating. The solid lines represent the cases of bonded boundary, and the dash dot lines represent the cases of frictionless boundary. Representing the asymptotic values of effective modulus, the dashed lines were calculated using the solutions presented in Refs. [14,21] for the case of a rigid inclusion translation with radius R_c in the matrix (i.e., shear modulus G_m and Poisson ratio ν_m). $\nu_c = 0.3$ and $\nu_m = 0.3$ are chosen in this figure.

4.2 Estimation of Coating Stiffness. A practical application of the present solution is to estimate the modulus of the coating. This requires an estimate of the coating Poisson ratio, ν_c , a measurement of G_{eff} from an experimental force–displacement relationship, a measurement of bead diameter R_i and coating outer diameter R_c from microscopy, and an independent measurement of matrix mechanical properties (G_m and ν_m) from a standard tensile test.

Solving G_c in Eq. (18) for the case of a perfectly bonded coating yielded

$$\frac{G_c}{G_m} = \frac{SX_1 + (G_{\text{eff}}/G_m)X_4 + \sqrt{((SX_1 + (G_{\text{eff}}/G_m)X_4)^2 - 4(G_{\text{eff}}/G_m)X_3(SX_2 + (G_{\text{eff}}/G_m)X_5))}}{2(-SX_2 - (G_{\text{eff}}/G_m)X_5)} \quad (28)$$

and, analogously, solving Eq. (26) for G_c for the case of frictionless boundary yielded

$$\frac{G_c}{G_m} = \frac{SY_1 + (G_{\text{eff}}/G_m)Y_4 + \sqrt{((SY_1 + (G_{\text{eff}}/G_m)Y_4)^2 - 4(G_{\text{eff}}/G_m)Y_3(SX_2 + (G_{\text{eff}}/G_m)Y_5))}}{2(-SY_2 - (G_{\text{eff}}/G_m)Y_5)} \quad (29)$$

Note that X_1, X_3, X_4 and Y_2, Y_3, Y_5 approach zero when $R_c/R_i \rightarrow 1$, which means that the right-hand side of Eq. (28) approaches zero and the right-hand side of Eq. (29) approaches infinity when $R_c/R_i \rightarrow 1$. Both of these limiting cases are meaningless, for G_c/G_m (i.e., β) disappears in Eqs. (18) and (26) when $R_c/R_i \rightarrow 1$. Correspondingly, Eqs. (18) and (26) become “artificial” equations for G_c/G_m . That is, solutions (28) and (29) are meaningless when $R_c/R_i \rightarrow 1$.

Plotting Eqs. (28) and (29) as a function of G_{eff}/G_m for $\nu_c = \nu_m = 0.3$ and for a range of coating thicknesses revealed monotonic trends (Fig. 3). An asymptote at which the coating is effectively rigid was observed. The effect of coating stiffness on the trends in Fig. 3 was again for perfect bonding to increase the resistance of the bead to displacement; failing to account for bead-coating sliding will lead to underestimation of the coating stiffness.

4.3 Application to Estimation of Cytoplasmic Stiffness. We next explored whether the approach could be effective for the purpose of estimating the effective elastic modulus of cytoplasm, as has been the goal of papers cited above dating as far back as the early 1920s [25]. The idea here is that a magnetic bead would be embedded in the cytoplasm of a cell and displaced by magnetic force or that the entire nucleus of a cell with a relatively rigid, highly lamin-coated nucleus would be displaced by a bead on its interior. The lamin network surrounding the nucleus can be sufficiently stiff to impeded cell migration [26]. The bead or nucleus itself would function as the rigid sphere, the cytoplasm as the coating, and the extracellular matrix or hydrogel as the infinite matrix. Although these conditions are not representative of natural tissues, they are realistic for model systems with both natural and synthetic extracellular matrices, bespoke systems typically designed for the specific purpose of quantifying cellular biophysics [8]. Magnetic activation

is common for such systems [27], and the tracking of bead displacements in three dimensions for the purpose of measuring cell biophysics is commonplace [28].

The results of Sec. 4.2 indicated that in certain regions of parameter space, the modulus of a coating can be estimated with high resolution, while in others the resolution is low. For the cases of interest here, the cytoplasm would be expected to be much more compliant than the matrix: estimates of cytoplasmic stiffness from bead rheology experiments are in the order of 10–1000 Pa [29], while moduli of collagen are in the order of 1–300 MPa [30]. For G_c/G_m in this range and below, the relationship between G_{eff}/G_m and G_c/G_m is linear (Fig. 4). The range of linearity terminates at an upper value of G_c/G_m that increases with decreasing bead or nucleus size R_c/R_i . For $R_c/R_i=2$, corresponding to the volume of the bead or nucleus is about 10% of the whole volume of the coating and bead (or nucleus), the range extends up to $G_c/G_m \ll 0.1$. Within the linear range, the coating modulus relates to the effective modulus according to

$$G_c = \eta^* G_{\text{eff}} \quad (30)$$

where

$$\eta^* = \begin{cases} \frac{X_3}{X_1 S^3}, & \text{fully bonded bead/coating interface} \\ \frac{Y_3}{Y_1 S^3}, & \text{frictionless bead/coating interface} \end{cases} \quad (31)$$

When the modulus of the coating is sufficiently small compared to that of the matrix, the matrix is essentially rigid and G_{eff} depends on the size and mechanical properties of the coating (shear modulus, Poisson's ratio, and thickness); the mechanical properties of the matrix do not affect the amount that the bead displaces. For example, for the case of a perfectly bonded bead-coating interface in the linear range,

$$\eta^* = \frac{(\alpha - 1)^2}{48\alpha(1 - \nu_c)(\alpha^5 - 1)(4 - 6\nu_c)} [4(1 + \alpha^4)(-2 + 3\nu_c)(-5 + 6\nu_c) + \alpha(1 + \alpha^2)(35 - 108\nu_c + 72\nu_c^2) + 6\alpha^2(5 - 18\nu_c + 12\nu_c^2)] \quad (32)$$

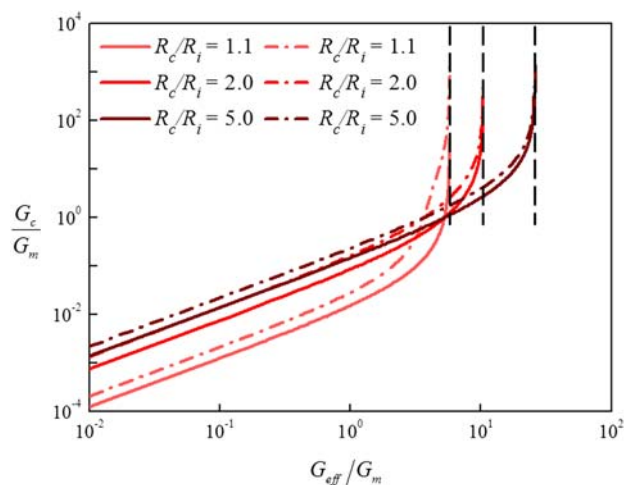


Fig. 4 Determination of the stiffness ratio between the coating and matrix by the effective modulus. Different trends represent different radii of the coating. The solid lines represent the cases of bonded boundary, and the dash dot lines represent the cases of frictionless boundary. The dash lines represent the limit values of effective modulus. $\nu_c = 0.3$ and $\nu_m = 0.3$ are chosen in this figure.

4.4 Implications for the Role of Nuclear Lamination in Nuclear Mechanosensing. The nucleus of animal cells connects through the cytoplasm to the extracellular matrix (ECM) through an integrated network of proteins called the LINC complex [31]. This complex determines the degree to which cytoskeletal stress, either from external loading or internal contraction, delivers mechanical force to the nuclear envelope. Proteins of the lamin family surrounding the nucleus form over the course of development and can form a shell that is stiff over certain time scales of loading [32]. The degree to which the nucleus translates in response to an applied force relates to the degree to which the nucleus can be perturbed by stressing of the ECM.

Equations (30) and (31) have certain consequences for cellular mechanosensing. First, the time scales over which nuclear mechanosensing via the LINC complex can occur must change as the short-term mechanical stiffness of the nucleus changes: as lamination progresses and the nuclear envelope stiffens, the nucleus ceases to sense the ECM stiffness and instead senses only the cytoskeleton and cytoplasm. Changes to cell and ECM stiffness over development, wound healing, and aging [33], thus, can serve as tools with which to affect how the nucleus senses exogenous mechanical force over longer time scales, and cytoskeletal fluidization in response to rapidly applied forces [34] can do so over shorter time scales.

An additional aspect of potential nuclear mechanosensing on which this solution sheds light is the controversial possibility of mechanical vibration affecting cell function. Cells including osteoblasts have been reported to respond favorably to certain frequencies of mechanical vibration [35]. In osteoblasts, the reported outcome is upregulation of the deposition of new bone tissue. A central question that must be answered if this is to occur is how information about vibration can make it through the ECM to change gene expression and thereby upregulate bone deposition. Why could this occur in bones but not in tendons? From the perspective of the current solution, if the ECM is sufficiently stiff compared to the cytosol, the nucleus could vibrate in a way that depends on the mechanics of the cytosol and cytoskeleton only. This means that, provided that the mechanical signal is sufficiently strong that viscous attenuation does not damp it entirely, a signal tuned to reach the nucleus could possibly penetrate the ECM to engage nuclear mechanosensing. For $R_c/R_i=2$ and $G_c/G_m \leq 0.1$, the effective stiffness for nuclear displacement is well within the range that depends linearly on the stiffness of the cytosol (Fig. 4).

5 Conclusions

The solution presented for the displacement of a coated, rigid bead within an elastic matrix enables the characterization of the shear modulus of a coating on a bead that is displaced via optical or magnetic actuation. For cases of a matrix that is relatively stiff compared to the coating, the bead feels only the coating and is insulated from the matrix. For cases of a matrix that is more compliant, the effect of the coating and matrix combine nonlinearly. The results have implications for magnetic testing of biological materials and for ways that the cell nucleus might respond to vibratory loading.

Acknowledgment

This work was supported by the National Natural Science Foundation of China (NNSFC) (11372243, 11522219, 11532009), the National Institutes of Health through Grant No. U01EB016422, and the National Science Foundation (NSF) through the Science and Technology Center for Engineering Mechanobiology (Grant No. CMMI 1548571).

Appendix A: Coefficients in the analytic solution

The coefficients in Eqs. (12) and (13) are given by

$$A_0^{(c)} = \frac{Z_0 + Z_1\beta + Z_2\beta^2}{X_3 + X_4\beta + X_5\beta^2} U$$

$$A_1^{(c)} = \frac{3U}{2R^2} \frac{\alpha(\alpha^2 - 1)(1 - \beta)(1 - \nu_m)}{X_3 + X_4\beta + X_5\beta^2}$$

$$A_2^{(c)} = 3RU \frac{\alpha(1 - \nu_m)\{2(\alpha^5 - 1)(2 - 3\nu_c) + \beta[2(2 - 3\nu_c) + \alpha^5(1 + \nu_c)]\}}{X_3 + X_4\beta + X_5\beta^2}$$

$$A_3^{(c)} = R^3 U \frac{\alpha^3(1 - \nu_m)\{2(\alpha^3 - 1)(2 - 3\nu_c) + \beta[2(2 - 3\nu_c) + \alpha^3(1 + \nu_c)]\}}{X_3 + X_4\beta + X_5\beta^2}$$

and

$$A_2^{(m)} = 3RU \frac{\alpha\beta(1 - \nu_m)\{2(\alpha^5 - 1)(2 - 3\nu_c) + \beta[2(2 - 3\nu_c) + \alpha^5(1 + \nu_c)]\}}{X_3 + X_4\beta + X_5\beta^2}$$

$$A_3^{(m)} = R^3 U \frac{\alpha^3\beta(1 - \nu_c)\{4(\alpha^3 - 1) + \alpha^3(\alpha^2 - 1)(5\nu_m - 1) - 6\nu_1(\alpha^5 - 1) + \beta[4 - 6\nu_c + \alpha^5(1 + \nu_c)]\}}{X_3 + X_4\beta + X_5\beta^2}$$

where

$$\alpha = \frac{R_c}{R_i}, \beta = \frac{G_c}{G_m}$$

$$X_3 = (\alpha - 1)^2(1 - \nu_m)[4(1 + \alpha^4)(2 - 3\nu_c)(5 - 6\nu_c) + \alpha(1 + \alpha^2)(35 - 108\nu_c + 72\nu_c^2) + 6\alpha^2(5 - 18\nu_c + 12\nu_c^2)]$$

$$X_4 = (-1 + \alpha)\{4(2 - 3\nu_c)(10 - 11\nu_m - 11\nu_c + 12\nu_m\nu_c) + \alpha(1 + \alpha)[35 - 43\nu_m - 4\nu_c(5 - 6\nu_m)(5 - 3\nu_c)]$$

$$+ \alpha^3(1 + \alpha)[45 - 53\nu_m - 4\nu_c(5 - 6\nu_m)(5 - 3\nu_c)] + 2\alpha^5(1 - \nu_m)(1 + \nu_c)(5 - 6\nu_c)\}$$

$$X_5 = 2(5 - 6\nu_m)(1 - \nu_c)[2(2 - 3\nu_c) + \alpha^5(1 + \nu_c)]$$

$$Z_0 = (1 - \alpha)(1 - \nu_m)[4(2 - 3\nu_c)(5 - 6\nu_c)(1 + \alpha + \alpha^2 + \alpha^3 + \alpha^4) + 5\alpha^3(1 + \alpha)]$$

$$Z_1 = 4(-2 + 3\nu_c)(10 - 11\nu_m - 11\nu_c + 12\nu_m\nu_c) + \alpha^3(-5 + 5\nu_m) + \alpha^5(35 - 43\nu_m - 98\nu_c + 118\nu_m\nu_c + 72\nu_c^2 - 84\nu_m\nu_c^2)$$

$$Z_2 = 2(-5 + 6\nu_m)(-1 + \nu_c)[2(2 - 3\nu_c) + \alpha^5(1 + \nu_c)]$$

The coefficients in Eqs. (21) and (22) are

$$B_0^{(c)} = \frac{W_0 + W_1\beta + W_2\beta^2}{Y_3 + Y_4\beta + Y_5\beta^2} U$$

$$B_1^{(c)} = \frac{3U}{2R_i^2} \frac{\alpha(1 - \beta)(1 - \nu_m)(1 + \alpha^2 - 2\nu_c)}{Y_3 + Y_4\beta + Y_5\beta^2}$$

$$B_2^{(c)} = 3R_i U \frac{\alpha(1 - \nu_m)[\beta(\alpha^5 - 1)(1 + \nu_c) + 1 + \nu_c + 2\alpha^5(2 - 3\nu_c)]}{Y_3 + Y_4\beta + Y_5\beta^2}$$

$$B_3^{(c)} = R_i^3 U \frac{\alpha^3(1 - \nu_m)[1 - 4\alpha^3 + \nu_c + 14\alpha^3\nu_c - 12\alpha^3\nu_c^2 + \beta(1 + \nu_c)(-1 - \alpha^3 + 2\alpha^3\nu_c)]}{Y_3 + Y_4\beta + Y_5\beta^2}$$

and

$$B_2^{(m)} = 3R_i U \frac{\alpha\beta(1 - \nu_c)[1 + \nu_c + 2\alpha^5(2 - 3\nu_c) + \beta(\alpha^5 - 1)(1 + \nu_c)]}{Y_3 + Y_4\beta + Y_5\beta^2}$$

$$B_3^{(m)} = R_i^3 U \frac{\alpha^3\beta(1 - \nu_c)[1 + \nu_c + 2\alpha^5(2 - 3\nu_c) + \beta(\alpha^5 - 1)(1 + \nu_c)]}{Y_3 + Y_4\beta + Y_5\beta^2}$$

where

$$\alpha = \frac{R_c}{R_i}, \beta = \frac{G_c}{G_m}$$

$$Y_3 = (\alpha - 1)(1 - \nu_m)[2(1 + \nu_c)(5 - 6\nu_c) + \alpha(1 + \alpha)(1 - 20\nu_c + 24\nu_c^2) + \alpha^3(1 + \alpha)(11 - 40\nu_c + 24\nu_c^2) + 4\alpha^5(2 - 3\nu_c)(7 - 8\nu_c)]$$

$$Y_4 = 2(1 + \nu_c)(10 - 11\nu_m - 11\nu_c + 12\nu_m\nu_c) - 9\alpha(1 - \nu_m)(1 + 2\nu_c - 4\nu_c^2)$$

$$+ 10\alpha^3(1 - \nu_m)(1 - 2\nu_c) + \alpha^5(35 - 43\nu_m - 98\nu_c + 118\nu_m\nu_c) + 72\nu_c^2 - 84\nu_m\nu_c^2 + 2\alpha^6(1 - \nu_m)(1 + \nu_c)(7 - 8\nu_c)$$

$$Y_5 = 2(\alpha^5 - 1)(5 - 6\nu_m)(1 - \nu_c)(1 + \nu_c)$$

$$W_0 = (-1 + \nu_c)[-2(1 + \nu_c)(-5 + 6\nu_c) + 5\alpha^3(1 - 2\nu_c) + 9\alpha^5(5 - 12\nu_c + 8\nu_c^2)]$$

$$W_1 = 2(1 + \nu_c)(10 - 11\nu_m - 11\nu_c + 12\nu_m\nu_c) + 5\alpha^3(-1 + \nu_m)(-1 + 2\nu_c) + \alpha^5(35 - 43\nu_m - 98\nu_c + 118\nu_m\nu_c + 72\nu_c^2 - 84\nu_m\nu_c^2)$$

$$W_2 = 2(-1 + \alpha)(1 + \alpha + \alpha^2 + \alpha^3 + \alpha^4)(-5 + 6\nu_m)(-1 + \nu_c)(1 + \nu_c)$$

Appendix B: Degradation details of the coated inclusion translation problem

In this appendix, we will reduce the coated inclusion translation problem to the classical Robin problem in the appropriate limits, including coating with no material mismatch ($\nu_c = \nu_m$, $G_c = G_m$) and coating with no thickness ($R_c/R_i = 1$).

Case 1: Coating with no material mismatch ($\nu_c = \nu_m$, $G_c = G_m$ or $\nu_c = \nu_m$, $\beta = 1$).

(i) Bonded sphere-coating interface

In this case, upon calculating directly the coefficients appearing in Appendix A, we arrive at

$$\lim_{\beta \rightarrow 1, \nu_c \rightarrow \nu_m} A_0^{(c)} = 0$$

$$\lim_{\beta \rightarrow 1, \nu_c \rightarrow \nu_m} A_1^{(c)} = 0$$

$$\lim_{\beta \rightarrow 1, \nu_c \rightarrow \nu_m} A_2^{(c)} = \frac{3UR_i}{2(5 - 6\nu_m)}$$

$$\lim_{\beta \rightarrow 1, \nu_c \rightarrow \nu_m} A_3^{(c)} = \frac{UR_i^3}{2(5 - 6\nu_m)}$$

$$\lim_{\beta \rightarrow 1, \nu_c \rightarrow \nu_m} A_2^{(m)} = \frac{3UR_i}{2(5 - 6\nu_m)}$$

$$\lim_{\beta \rightarrow 1, \nu_c \rightarrow \nu_m} A_3^{(m)} = \frac{UR_i^3}{2(5 - 6\nu_m)}$$

which are identical to the solutions presented in Refs. [12,14,21].

(ii) Frictionless sphere-coating interface

Direct calculation for the coefficients in Appendix A leads to

$$\lim_{\beta \rightarrow 1, \nu_c \rightarrow \nu_m} B_0^{(c)} = 0$$

$$\lim_{\beta \rightarrow 1, \nu_c \rightarrow \nu_m} B_1^{(c)} = 0$$

$$\lim_{\beta \rightarrow 1, \nu_c \rightarrow \nu_m} B_2^{(c)} = \frac{3UR_i}{2(7 - 8\nu_m)}$$

$$\lim_{\beta \rightarrow 1, \nu_c \rightarrow \nu_m} B_3^{(c)} = \frac{UR_i^3(-1 + 2\nu_m)}{2(7 - 8\nu_m)}$$

$$\lim_{\beta \rightarrow 1, \nu_c \rightarrow \nu_m} B_2^{(m)} = \frac{3UR_i}{2(7 - 8\nu_m)}$$

$$\lim_{\beta \rightarrow 1, \nu_c \rightarrow \nu_m} B_3^{(m)} = \frac{UR_i^3(-1 + 2\nu_m)}{2(7 - 8\nu_m)}$$

which is the same as the solution presented in Ref. [14].

Case 2: Coating with no thickness ($R_c/R_i = 1$ or $\alpha = 1$).

(i) Bonded sphere-coating interface.

In the limit $\alpha = 1$, it follows from Appendix A that

$$\lim_{\alpha \rightarrow 1} A_0^{(c)} = \frac{U\{5(-1 + \beta) + (5 - 6\beta)\nu_m + \nu_c[6 - 5\beta + 6(-1 + \beta)\nu_m]\}}{\beta(-1 + \nu_c)(-5 + 6\nu_m)}$$

$$\lim_{\alpha \rightarrow 1} A_1^{(c)} = 0$$

$$\lim_{\alpha \rightarrow 1} A_2^{(c)} = -\frac{3UR_i(-1 + \nu_m)}{2\beta(-1 + \nu_c)(-5 + 6\nu_m)}$$

$$\lim_{\alpha \rightarrow 1} A_3^{(c)} = -\frac{UR_i^3(-1 + \nu_m)}{2\beta(-1 + \nu_c)(-5 + 6\nu_m)}$$

$$\lim_{\alpha \rightarrow 1} A_2^{(m)} = \frac{3UR_i}{2(5 - 6\nu_m)}$$

$$\lim_{\alpha \rightarrow 1} A_3^{(m)} = \frac{UR_i^3}{2(5 - 6\nu_m)}$$

which are the same as the solutions presented in Refs. [12,14,21].

(ii) Frictionless sphere-coating interface

In the limit $\alpha = 1$, it follows from Appendix A that

$$\lim_{\alpha \rightarrow 1} B_0^{(c)} = \frac{U\{6(-1 + \beta) + (6 - 7\beta)\nu_m + \nu_c[6 - 5\beta + 6(-1 + \beta)\nu_m]\}}{\beta(-1 + \nu_c)(-7 + 8\nu_m)}$$

$$\lim_{\alpha \rightarrow 1} B_1^{(c)} = \frac{3U(-1 + \beta)(-1 + \nu_m)}{10\beta R_i^2(-1 + \nu_c)(-7 + 8\nu_m)}$$

$$\lim_{\alpha \rightarrow 1} B_2^{(c)} = -\frac{3UR_i(-1 + \nu_m)}{2\beta(-1 + \nu_c)(-7 + 8\nu_m)}$$

$$\lim_{\alpha \rightarrow 1} B_3^{(c)} = \frac{UR_i^3[3 + 2\beta + 2(-6 + \beta)\nu_c](-1 + \nu_m)}{10\beta(-1 + \nu_c)(-7 + 8\nu_m)}$$

$$\lim_{\alpha \rightarrow 1} B_2^{(m)} = \frac{3UR_i}{2(-7 + 8\nu_m)}$$

$$\lim_{\alpha \rightarrow 1} B_3^{(m)} = \frac{UR_i^3(-1 + 2\nu_m)}{2(-7 + 8\nu_m)}$$

Because the thickness of the coating approaches zero, it is sufficient to focus on the solution in the matrix. This reduced solution in the matrix is the same as the solution given in Ref. [14].

References

- [1] Freundlich, H., and Seifriz, W., 1923, "Ueber die elastizität von solen und gelen," *Z. Phys. Chem.*, **104**(1), pp. 233–261.
- [2] Kupradze, V. D. (1965). *Potential Methods in the Theory of Elasticity*, Israel Program for Scientific Translations, Jerusalem.
- [3] Lurie, A., and Belyaev, A., 2005, *Theory of Elasticity (Foundations of Engineering Mechanics)*, Springer, Berlin, pp. 978–973.
- [4] De, V. L., and Dekker, C., 2012, "Recent Advances in Magnetic Tweezers," *Annu. Rev. Biophys.*, **41**(1), pp. 453–472.
- [5] Lefèvre, V., Danas, K., and Lopezpamies, O., 2017, "A General Result for the Magnetoelastic Response of Isotropic Suspensions of Iron and Ferrofluid Particles in Rubber. With Applications to Spherical and Cylindrical Specimens," *J. Mech. Phys. Solids*, **107**, pp. 343–364.
- [6] Zhong, Q. Y., and Selvadurai, A. P. S., 1995, "On the Mechanics of a Rigid Disc Embedded in a Fluid Saturated Poroelastic Medium," *Int. J. Eng. Sci.*, **33**(11), pp. 1633–1662.
- [7] Giordano, S., Palla, P. L., Cadelano, E., and Brun, M., 2012, "Elastic Behavior of Inhomogeneities With Size and Shape Different From Their Hosting Cavities," *Mech. Mater.*, **44**, pp. 4–22.
- [8] Huang, G., Li, F., Zhao, X., Ma, Y., Li, Y., Lin, M., Jin, G., Lu, T. J., Genin, G. M., and Xu, F., 2017, "Functional and Biomimetic Materials for Engineering of the Three-Dimensional Cell Microenvironment," *Chem. Rev.*, **117**(20), pp. 12764–12850.
- [9] Hooper, J. B., and Schweizer, K. S., 2006, "Theory of Phase Separation in Polymer Nanocomposites," *Macromolecules*, **39**(15), pp. 5133–5142.
- [10] Robin, G., 1886, "Sur la distribution de l'électricité à la surface des conducteurs fermés et des conducteurs ouverts," *Ann. Sci. Ecole Norm. Sup.*, **3**(2), pp. 31–358.
- [11] Lurie, A. I., 1967, "Elastostatic Robin Problem for a Triaxial Ellipsoid," *Mech. Solids*, **1**(2), pp. 80–83.
- [12] Selvadurai, A., 1975, "The Distribution of Stress in a Rubber-Like Elastic Material Bounded Internally by a Rigid Spherical Inclusion Subjected to a Central Force," *Mech. Res. Commun.*, **2**(3), pp. 99–106.
- [13] Zureick, A., 1988, "Transversely Isotropic Medium With a Rigid Spheroidal Inclusion Under an Axial Pull," *J. Appl. Mech.*, **55**, pp. 495–497.
- [14] Selvadurai, A. P. S., 2016, "Indentation of a Spherical Cavity in an Elastic Body by a Rigid Spherical Inclusion: Influence of Non-Classical Interface Conditions," *Continuum Mech. Thermodyn.*, **28**(1-2), pp. 617–632.
- [15] Lin, D. C., Yurke, B., and Langrana, N. A., 2005, "Use of Rigid Spherical Inclusions in Young's Moduli Determination: Application to DNA-Crosslinked Gels," *J. Biomech. Eng.*, **127**(4), pp. 571–579.
- [16] Selvadurai, A., 1976, "The Load-Deflection Characteristics of a Deep Rigid Anchor in an Elastic Medium," *Geotechnique*, **26**(4), pp. 603–612.
- [17] Kanwal, R., and Sharma, D., 1976, "Singularity Methods for Elastostatics," *J. Elast.*, **6**(4), pp. 405–418.
- [18] Hashin, Z., 1991, "The Spherical Inclusion With Imperfect Interface," *J. Appl. Mech.*, **58**(2), pp. 444–449.
- [19] Mura, T., and Furuhashi, R., 1984, "The Elastic Inclusion With a Sliding Interface," *J. Appl. Mech.*, **51**(2), pp. 308–310.
- [20] Kamgoué, A., Ohayon, J., and Tracqui, P., 2007, "Estimation of Cell Young's Modulus of Adherent Cells Probed by Optical and Magnetic Tweezers: Influence of Cell Thickness and Bead Immersion," *J. Biomech. Eng.*, **129**(4), pp. 523–530.

- [21] Walpole, L. J., 1991, "A Translated Rigid Ellipsoidal Inclusion in an Elastic Medium," *Proc. Math. Phys. Sci.*, **434**(1892), pp. 571–585.
- [22] Kachanov, M., Shafiro, B., and Tsukrov, I., 2003, *Handbook of Elasticity Solutions*, Kluwer Academic, Boston.
- [23] Eshelby, J. D., 1957, "The Determination of the Elastic Field of an Ellipsoidal Inclusion, and Related Problems," *Proc. R. Soc. A*, **241**(1226), pp. 376–396.
- [24] Lur'Ea, I., 1964, *Three-Dimensional Problems of the Theory of Elasticity*, Interscience Publishers, New York.
- [25] Rabinowitsch, B., 1929, "Über die viskosität und elastizität von solen," *Z. Phys. Chem.*, **145**(1), pp. 1–26.
- [26] Harada, T., Swift, J., Irianto, J., Shin, J.-W., Spinler, K. R., Athirasala, A., Diegmiller, R., Dingal, P. D. P., Ivanovska, I. L., and Discher, D. E., 2014, "Nuclear Lamin Stiffness Is a Barrier to 3D Migration, But Softness Can Limit Survival," *J. Cell Biol.*, **204**(5), pp. 669–682.
- [27] Li, Y., Hong, Y., Xu, G.-K., Liu, S., Shi, Q., Tang, D., Yang, H., Genin, G. M., Lu, T. J., and Xu, F., 2018, "Non-Contact Tensile Viscoelastic Characterization of Microscale Biological Materials," *Acta Mech. Sin.*, **34**(3), pp. 589–599.
- [28] Legant, W. R., Miller, J. S., Blakely, B. L., Cohen, D. M., Genin, G. M., and Chen, C. S., 2010, "Measurement of Mechanical Traction Exerted by Cells in Three-Dimensional Matrices," *Nat. Methods*, **7**(12), pp. 969–971.
- [29] Yamada, S., Wirtz, D., and Kuo, S. C., 2000, "Mechanics of Living Cells Measured by Laser Tracking Microrheology," *Biophys. J.*, **78**(4), pp. 1736–1747.
- [30] Marquez, J. P., Genin, G. M., Zahalak, G. I., and Elson, E. L., 2005, "The Relationship Between Cell and Tissue Strain in Three-Dimensional Bio-Artificial Tissues," *Biophys. J.*, **88**(2), pp. 778–789.
- [31] Crisp, M., Liu, Q., Roux, K., Rattner, J., Shanahan, C., Burke, B., Stahl, P. D., and Hodzic, D., 2006, "Coupling of the Nucleus and Cytoplasm: Role of the LINC Complex," *J. Cell Biol.*, **172**(1), pp. 41–53.
- [32] Swift, J., Ivanovska, I. L., Buxboim, A., Harada, T., Dingal, P. D. P., Pinter, J., Pajerowski, J. D., Spinler, K. R., Shin, J.-W., and Tewari, M., 2013, "Nuclear Lamin-A Scales with Tissue Stiffness and Enhances Matrix-Directed Differentiation," *Science*, **341**(6149), p. 1240104.
- [33] Babaei, B., Davarian, A., Lee, S.-L., Pryse, K. M., McConnaughey, W. B., Elson, E. L., and Genin, G. M., 2016, "Remodeling by Fibroblasts Alters the Rate-Dependent Mechanical Properties of Collagen," *Acta Biomater.*, **37**, pp. 28–37.
- [34] Trepat, X., Deng, L., An, S. S., Navajas, D., Tschumperlin, D. J., Gerthoffer, W. T., Butler, J. P., and Fredberg, J. J., 2007, "Universal Physical Responses to Stretch in the Living Cell," *Nature*, **447**(7144), pp. 592–595.
- [35] Tirkkonen, L., Halonen, H., Hyttinen, J., Kuokkanen, H., Sievanen, H., Koivisto, A. M., Mannerstrom, B., Sandor, G. K., Suuronen, R., Miettinen, S., and Haimi, S., 2011, "The Effects of Vibration Loading on Adipose Stem Cell Number, Viability and Differentiation Towards Bone-Forming Cells," *J. R. Soc. Interface*, **8**(65), pp. 1736–1747.